Galvanostatic Ion De-Trapping Rejuvenates Oxide Thin Films

Miguel A. Arvizu,[†] *Rui-Tao Wen,**[,†] *Daniel Primetzhofer,*[‡] *Jolanta E. Klemberg-Sapieha,*[§] *Ludvik Martinu,*[§] *Gunnar A. Niklasson,*[†] *and Claes G. Granqvist* [†]

[†]Department of Engineering Sciences, The Ångström Laboratory, Uppsala University, P. O. Box 534, SE-751 21 Uppsala, Sweden

[‡]Department of Physics and Astronomy, Ion Physics, Uppsala University, P. O. Box 516, SE-751 20 Uppsala, Sweden

[§]Department of Engineering Physics, École Polytechnique de Montréal, P. O. Box 6079, Montreal, Quebec H3C 3A7, Canada

Keywords: Smart windows, WO_3, electrochromism, ion de-trapping, ToF-ERDA

ABSTRACT

Ion trapping under charge insertion–extraction is well known to degrade the electrochemical performance of oxides. Galvanostatic treatment was recently shown capable to rejuvenate the oxide, but the detailed mechanism remained uncertain. Here we report on amorphous electrochromic (EC) WO_3 thin films prepared by sputtering and electrochemically cycled in a lithium-containing electrolyte under conditions leading to severe loss of charge exchange capacity and optical modulation span. Time-of-Flight Elastic Recoil Detection Analysis (ToF-ERDA) documented pronounced Li^+ trapping associated with the degradation of the EC properties and, importantly, that Li^+ de-trapping, caused by a weak constant current drawn through the film for some time, could recover the original EC performance. Thus ToF-ERDA provided direct and unambiguous evidence for Li^+ de-trapping.

*Email: Ruitao.Wen@angstrom.uu.se

Electrochromic (EC) materials are able to change their optical properties under the action of an electric field or current.[1,2] The largest application, at least with regard to surface area, is for EC architectural "smart widows" capable of providing energy efficiency in actively cooled buildings and simultaneously yielding comfortable indoor conditions.[3-5] EC devices for these applications typically use a WO_3 thin film separated from a Ni-oxide-based thin film by an ion-conductor, usually for Li^+, in thin-film form or being a layer of a polymer electrolyte, and electrical powering is made possible by embedding this three-layer configuration between thin films of transparent electrical conductors.[5-7] Optical modulation ensues when ions are shuttled between the WO_3 film, which colors cathodically by ion insertion, and the Ni-oxide-based film with complementary anodic coloration under ion extraction.[8] Large optical modulation span is required for most EC devices, which means that the inserted and extracted ion densities are also large, and this may lead to device degradation due to irreversible ion incorporation as well as structural rearrangements.

Durability under repeated ion insertion and extraction is of obvious interest for EC devices. We have recently studied this feature for WO_3 films and argued that the degradation was associated with ion trapping,[9] which is in line with current theoretical ideas.[10-13] Importantly, we also discovered that the WO_3-based films could be brought back to their initial conditions by running a weak constant current through bleached films for several hours; *i.e.*, galvanostatic rejuvenation was possible.[9] Optical data on WO_3 films with different levels of Li^+ trapping, and the relation of these data to detailed results from the literature,[14] led us to the tentative conclusion that Li^+ trapping took place and that the galvanostatic treatment yielded Li^+ de-trapping. Here we are able to demonstrate direct evidence for Li^+ trapping and de-trapping by use of Time-of-Flight Elastic Recoil Detection Analysis (ToF-ERDA).

Amorphous thin films of WO_3 were prepared by reactive dc magnetron sputtering, *i.e.*, by an industrially viable and scalable technique[15] which is in widespread use for making EC

"smart windows".[5] The substrate was a glass plate precoated with a transparent and electrically conducting layer of In_2O_3:Sn (known as ITO). The same technique was used in earlier work of ours[9,16] and is described, along with other technical details, in Supplementary Information. WO_3 films with thicknesses of 300 ± 10 nm were immersed in an electrolyte of $LiClO_4$ in propylene carbonate (denoted as Li–PC), and were electrochemically cycled 20 times in a potential range as wide as 1.5–4.0 V vs. Li/Li^+ at 10 mV/s in order to rapidly induce severe degradation. The open circuit potential (OCP) decreased from 3.5 V to 1.95 V after 20 cycles. **Figure 1**a shows selected data from cyclic voltammetry (CV) which confirm the strong, progressive decline of the charge density exchange, and Figures 1b and 1c indicate specific data on charge density Q during ion insertion and extraction and on the difference δQ between inserted and extracted charge during each CV cycle, defined as $\delta Q = \left| Q_{\text{Inserted}} + Q_{\text{Extracted}} \right|$. Data in Figure 1c are qualitatively similar to those shown before[16] but the degradation, which is peaked after five CV cycles, is much faster as a consequence of the wider potential range. Analogous experiments were performed for WO_3 thin films with different thickness (Figure S1), and it was verified that the cycle-dependent charge density exchange scaled with the film thickness. **Figure 2**a reports corresponding optical transmittance spectra in the $400 < \lambda < 800$ nm wavelength range, encompassing visible light, and shows that the optical modulation is lost in a way that is consistent with the decline in the CV data. Monochromatic transmittance for λ = 550 nm—*i.e.*, at the peak in the eye's sensitivity—is depicted in Figure 2b and reiterates the pronounced degradation during 20 CV cycles.

After completing the CV cycling, we applied a constant current density of 1×10^{-5} A cm^{-2} for 20 h with the aim of rejuvenating the EC properties. Figure 2c shows the concomitant evolution of the voltage as a function of time; the results are similar to those shown before.[9] Correspondingly, the optical properties returned to the original ones, as seen in Figure 2a. The

minor differences at short wavelengths are ascribed to ions that are irreversibly trapped in energetically deep states.[9] We notice some erratic structure and plateaus in the voltage *vs*. time in Figure 2c and analogously some irregular structure in the monochromatic transmittance *vs*. time between stages II and III in Figure 2b. We believe that the major transmittance increase after ~9 h is associated with complete Li^+ de-trapping, but we are presently unable to account for the abruptness and magnitude of the increase. The transmittance at λ = 550 nm reached the initial value after about 17 h. After turning off the current load, the OCP was recorded for some hours and asymptotically reached ~3.5 V *vs*. Li/Li^+; intriguingly, this value is identical to the initial OCP (Figure 2c). In order to elucidate any structure variation, we used X-ray diffraction (XRD) to study a WO_3 thin film in as-deposited state, after 20 CV cycles, and after rejuvenation. All XRD data were consistent with amorphous structures, as seen in Figure S2.

We now consider the quantitative Li content of WO_3 films in various states. Elemental depth profiling was accomplished with ToF-ERDA.[17] Three WO_3-based samples, corresponding to different stages of the CV cycling–rejuvenation process, were studied: as-deposited (I), after 20 CV cycles ending with the film in its bleached state (II), and after galvanostatic rejuvenation (III) (see Figure 2b). For comparison, we also studied a fourth sample that had been immersed for 12 h in the electrolyte without further treatment. **Figure 3**a shows elemental depth profiles for sample II, and part of the recorded time-of-flight/energy coincidence spectrum is presented in Figure 3b. Tracks for the individual masses are well separated for the materials of interest (*e.g.*, for ^6Li and ^7Li), and hence the data permit mass separation of the recoiling target atoms. Dashed lines in Figure 3b illustrate flight-times and energies corresponding to the film's surface (upper dashed line) and its interface to the substrate (lower dashed line). Elemental depth profiles clearly show high concentrations of Li as well as of the other expected thin-film constituents (W, O, and H) throughout the sample. A

weak signal from C can also be detected. The interface to the ITO layer is not clearly visible in ToF-ERDA owing to the similarity in mass for In, Sn and the primary ^{127}I ion. The approximate position of the ITO interface was determined separately by Rutherford Backscattering Spectroscopy and is shown by the left dashed vertical line in Figure 3a (labelled ITO). The signals from other elements (Na, Si, and Ca), observed at large depths, originate from the glass substrate, whose position is indicated by a second vertical dashed line (labelled Substrate). Limited energy resolution, as well as energy loss straggling of primary and recoiling particles, leads to the observed gradual increase in concentrations for the elements in the substrate as well as the gradual decrease of the signal from the thin film constituents.

Table 1 shows average concentrations of Li, W, O, H, and C for the four WO_3-based samples studied by ToF-ERDA. Average concentrations were obtained by excluding the near-surface region from a depth interval that extends until a level where the ITO interface is reached and/or substrate signals become significant. Some carbon contamination was noted. Figure 3c depicts actual Li depth profiles for differently treated samples. Clearly, the Li concentrations differ widely among the samples: Expectedly, no Li can be detected in the as-deposited sample (I), whereas its immersion in the electrolyte gives a low concentration. Running a sample through 20 CV cycles (II) yields as much as 18.3 at.% of Li, and galvanostatic rejuvenation (III) subsequently brings down the Li content to the ~1-at.%-level thus ascertaining successful de-trapping of Li ions. Light-ion concentrations in ToF-ERDA data can be subject to substantial systematic uncertainties (*e.g.*, ±25% of the recorded concentration for Li) due to limited detection efficiency, and relative comparisons between different samples is best done via concentration ratios (see Supporting Information).

The concentrations deduced for the other elements give some additional information. The O/W ratio is clearly modified when the Li concentration is increased and changes from ~3.6

to ~4.1 after 20 CV cycles and decreases to ~3.8 after galvanostatic rejuvenation. It is noteworthy that the deviation from the ideal stoichiometry (WO_3) matches the excess oxygen required to account for the observed H concentration in terms of hydroxide ions for samples with a low Li content.

Summarizing, we have used ToF-ERDA to demonstrate (*i*) that Li^+ intercalation can take place rather evenly throughout the cross-section of an electrochromic WO_3-based film, which is different from the case of electrochromic NiO-based films where the interaction with Li^+ is a surface phenomenon;[18] (*ii*) that the degradation of WO_3-based films under excessive voltammetric cycling is associated with Li^+ trapping; and (*iii*) that galvanostatic rejuvenation of WO_3 films is unambiguously related to Li^+ de-trapping. The results of this study are almost certainly applicable to other cathodically coloring electrochromic oxides[19], and possibly also to batteries and other types of ionics-based devices.

Supporting Information

The Supporting Information is available free of charge on the ACS Publications website

Acknowledgements

MAA thanks the Mexican Council for Science and Technology (CONACyT) for financial assistance (Scholarship No. 236561) to carry out postdoctoral research at Uppsala University. Our work was supported by the European Research Council under the European Community's Seventh Framework Program (FP7/2007–2013)/ERC Grant Agreement No. 267234 ("GRINDOOR").

References

(1) Granqvist, C. G. Electrochromic Materials: Out of a Niche. Nat. Mater. **2006**, 5, 89-90.

(2) Mortimer, R. J.; Rosseinsky, D. R.; Monk, P. M. S.; Electrochromic Materials and Devices. Wiley–VCH, Weinheim, Germany, **2015**.

(3) Deb, S. K. Opportunities and Challenges in Science and Technology of WO_3 for Electrochromic and Related Applications. Sol. Energ. Mater. Sol. Cells, **2008**, 92, 245-258.

(4) Gillaspie, D. T.; Tenent, R. C.; Dillon, A. C.; Metal-oxide Films for Electrochromic Applications: Present Technology and Future Directions. J. Mater. Chem. **2010**, 20, 9585-9592.

(5) Granqvist, C. G. Electrochromics for Smart Windows: Oxide-based Thin Films and Devices. Thin Solid Films **2014**, 564, 1-38.

(6) Ginley, D.; Hosono, H.; Paine, D. C.; editors, Handbook of Transparent Conductors. Springer Science + Business Media, New York, **2010**.

(7) Ellmer, K. Past Achievements and Future Challenges in the Development of Optically Transparent Electrodes. Nat. Photon. **2012**, 6, 809-817.

(8) Niklasson, G. A.; Granqvist, C. G.; Electrochromics for Smart Windows: Thin Films of Tungsten Oxide and Nickel Oxide, and Devices Based on These. *J. Mater. Chem.* **2007**, 17, 127-156.

(9) Wen, R.-T.; Granqvist, C. G.; Niklasson, G. A.; Eliminating Degradation and Uncovering Ion-trapping Dynamics in Electrochromic WO_3 Thin Films. *Nat. Mater.* **2015**, 14, 996-1001.

(10) Bisquert, J. Analysis of the Kinetics of Ion Intercalation: Ion Trapping Approach to Solid-state Relaxation Processes. Electrochim. Acta **2002**, 47, 2435-2449.

(11) Bisquert, J.; Vikhrenko, V. S.; Analysis of the Kinetics of Ion Intercalation. Two State Model Describing the Coupling of Solid State Ion Diffusion and Ion Binding Processes. *Electrochim. Acta* **2002**, 47, 3977-3988.

(12) Bisquert, J.; Fractional Diffusion in the Multiple-trapping Regime and Revision of the Equivalence with the Continuous-time Random Walk. *Phys. Rev. Lett.* **2003**, 91, 010602.

(13) Bisquert, J. Beyond the Quasistatic Approximation: Impedance and Capacitance of an Exponential Distribution of Traps. *Phys. Rev. B* **2008**, 77, 235203.

(14) Berggren, L.; Jonsson, J. C.; Niklasson, G. A. Optical Absorption in Lithiated Tungsten Oxide Thin Films: Experiment and Theory. *J. Appl. Phys.* **2007**, 102, 083538.

(15) Gläser, H. J. Large Area Glass Coating. von Ardenne Anlagentechnik GmbH, Dresden, Germany, **2000**.

(16) Arvizu, M. A.; Triana, C. A.; Stefanov, B. I.; Granqvist, C. G.; Niklasson, G. A. Electrochromism in Sputter-deposited W–Ti Oxide Films: Durability Enhancement Due to Ti. *Sol. Energ. Mater. Sol. Cells* **2014**, 125, 184-189.

(17) Zhang, Y.; Whitlow, H. J.; Winzell, T.; Bubb, I. F.; Sajavaara, T.; Arstila, K.; Keinonen, J. Detection efficiency of time-of-flight energy elastic recoil detection analysis systems. Nucl. Instr. Meth. Phys. Res. B **1999**, 149, 477-489.

(18) Wen, R.-T.; Granqvist, C. G.; Niklasson, G. A.; Anodic Electrochromism for Energy-Efficient Windows: Cation/Anion-Based Surface Processes and Effects of Crystal Facets in Nickel Oxide Thin Films. Adv. Funct. Mater. **2015**, 25, 3359-3370.

(19) Wen, R.-T.; Arvizu, M. A.; Niklasson, G. A.; Granqvist, C. G.; Electrochromics for Energy Efficient Buildings: Towards Long-term Durability and Materials Rejuvenation, Surf. Coat. Technol. **2015**, 278, 121–125

Figure 1. (a) Cyclic voltammetry (CV) data for a ~300-nm-thick WO_3 film immersed in Li–PC; data were taken after the indicated numbers of cycles. (b) Inserted and extracted charge density Q during voltammetric cycling, and (c) difference in charge density δQ for successive charge insertions and extractions as obtained from data shown in (a); symbols denoting data were joined by straight lines.

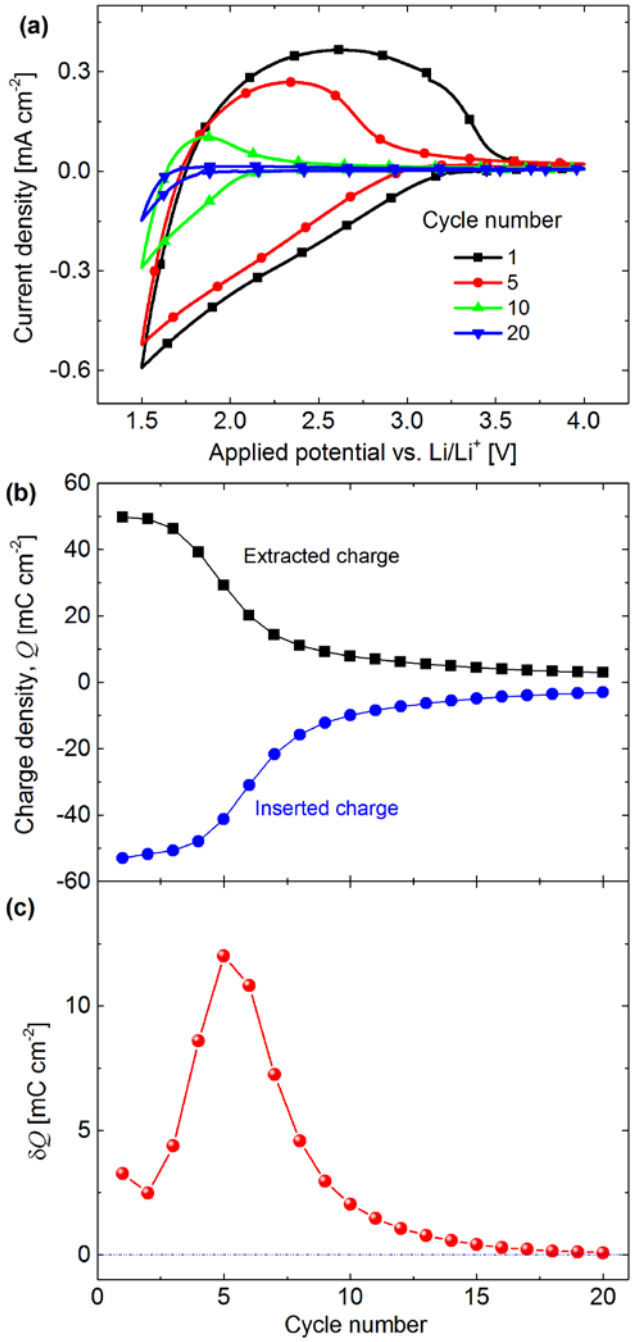

Figure 2. (a) Spectral transmittance for a ~300-nm-thick WO_3 film immersed in Li–PC; data were taken after the indicated numbers of voltammetric cycles and for the same film after having undergone rejuvenation by galvanostatic ion de-trapping. (b) Monochromatic transmittance at 550 nm during CV cycling at 1.5–4.0 V *vs*. Li/Li^+ and subsequent constant current loading; I, II and III are referred to in the main text. (c) Voltage *vs*. time during galvanostatic treatment followed by open circuit potential (OCP) measurements after the current load was aborted.

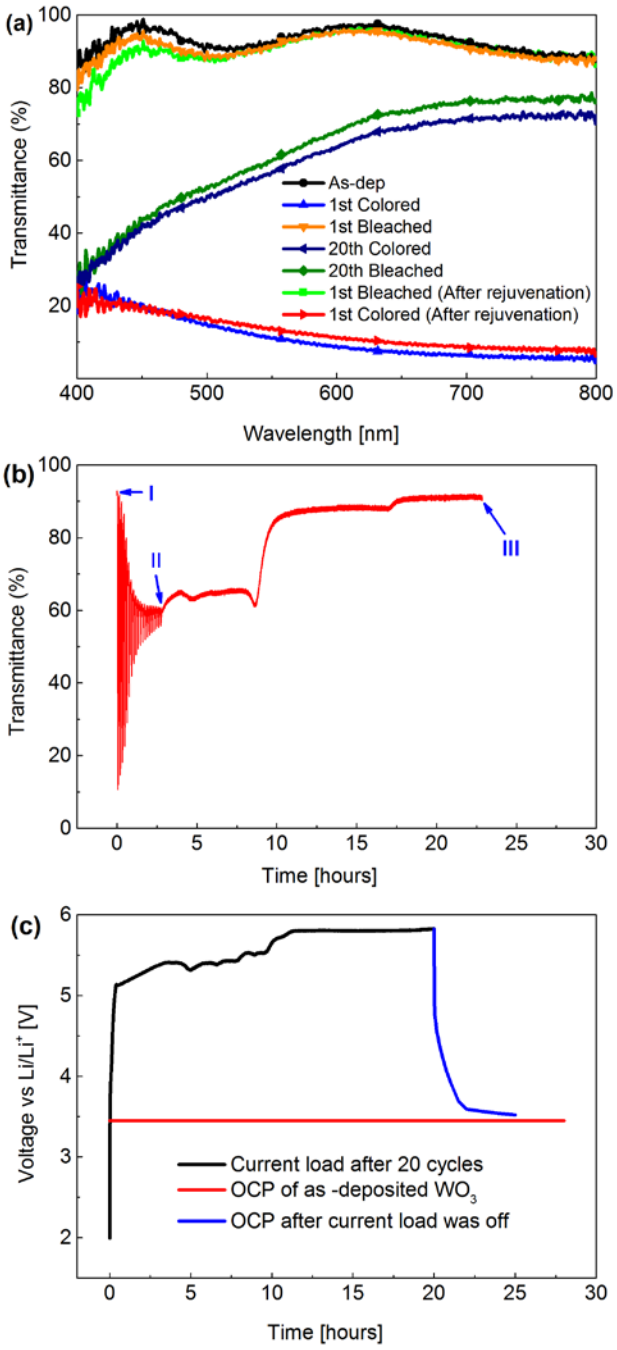

Figure 3. (a) Elemental depth profiles for a ~300-nm-thick WO_3 film subjected to 20 CV cycles in the range 1.5–4.0 V *vs*. Li/Li^+ and thereby severely degraded; the film was in its bleached state. (b) Time-of-flight/energy coincidence spectrum from which the information in (a) was reconstructed. Data were recorded for 36 MeV $^{127}I^{8+}$ primary ions and refers to the indicated elements. The vertical scale is a color-coded rendition of the number of coincidence events per pixel. (c) Li depth profiles for three differently treated samples. Further details are given in the main text.

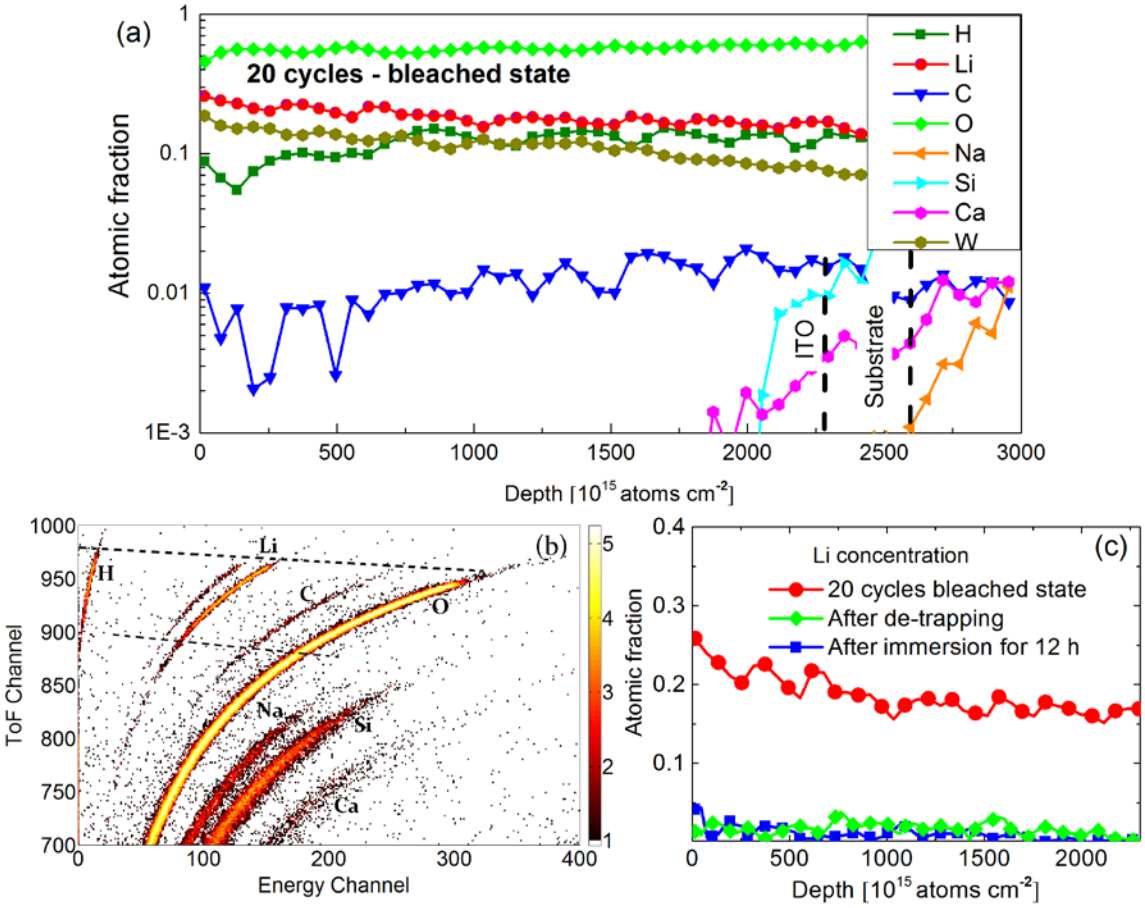

Table 1. Elemental contents for ~300-nm-thick WO_3-based samples in the indicated states.

Sample	Corresponding stage in Figure 2b	Element contents in *at*.%				
		Li	W	O	H	C
As-deposited	I	< 0.1	19.3	69.8	9.6	1.2
After 20 CV cycles, bleached	II	18.3	13.3	55.1	10.7	2.6
After rejuvenation	III	1.1	18.2	69.8	9.6	1.3
After immersion for 12 h	…	1.9	19.6	68.1	9.1	1.3

ToC Figure

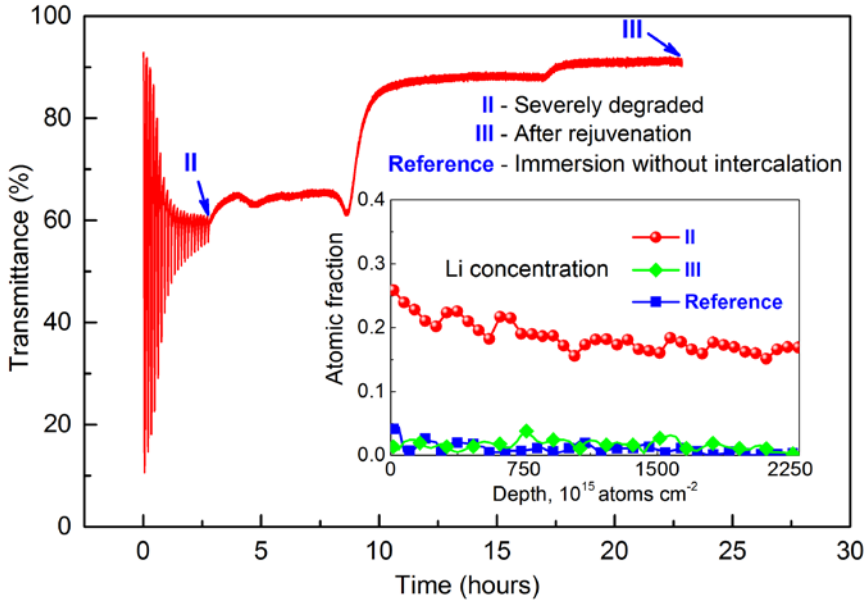
Transmittance (%)
Time (hours)
II
III
II - Severely degraded
III - After rejuvenation
Reference - Immersion without intercalation
Atomic fraction
Li concentration
II
III
Reference
Depth, 10^15 atoms cm^-2